NANO LETTERS

Letter

pubs.acs.org/NanoLett

Large Magnetoresistance through a Single Molecule due to a Spin-Split Hybridized Orbital

S. L. Kawahara,[†] J. Lagoute,*[,†] V. Repain,[†] C. Chacon,[†] Y. Girard,[†] S. Rousset,[†] A. Smogunov,[‡] and C. Barreteau[‡]

[†]Laboratoire Matériaux et Phénomènes Quantiques, UMR7162, Université Paris Diderot, Paris 7, Sorbonne Paris Cité, CNRS, UMR 7162 case courrier 7021, 75205 Paris 13, France

[‡]DSM/IRAMIS/SPCSI, CEA/Saclay, F-91191 Gif-sur-Yvette Cedex, France

Supporting Information

ABSTRACT: Using organic materials in spintronic devices raises a lot of expectation for future applications due to their flexibility, low cost, long spin lifetime, and easy functionalization. However, the interfacial hybridization and spin polarization between the organic layer and the ferromagnetic electrodes still has to be understood at the molecular scale. Coupling state-of-the-art spin-polarized scanning tunneling spectroscopy and spin-resolved ab initio calculations, we give the first experimental evidence of the spin splitting of a molecular orbital on a single non magnetic C_{60} molecule in contact with a magnetic material, namely, the Cr(001) surface. This hybridized molecular state is responsible for an inversion of sign of the tunneling magnetoresistance depending on energy. This result opens the way to spin filtering through molecular orbitals.

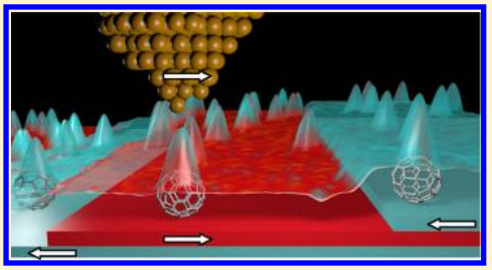

KEYWORDS: *Spin-polarized STM, fullerene, molecular orbital, density functional theory*

Spintronics is a quantum electronics which exploits the spin degree of freedom of the electron rather than or in addition to its charge. Since the two key discoveries of spin polarized tunneling in 1971[1] and giant magnetoresistance in 1987,[2] this field of research has considerably grown and raised the hope for more efficient devices of data storage and computing. Spintronics tunneling devices lie on a multilayer geometry where an insulating spacer is sandwiched between two magnetic materials.[3] This tunnel barrier can be an inorganic semiconducting layer, which has been shown to exhibit very long spin lifetime,[4,5] but an advantageous alternative route for applications is the use of organic molecules.[6,7] Recently, magnetoresistive devices with molecules have shown unexpectedly large magnetoresistances.[7,8] A spin transport model that describes the role of interfacial spin-dependent metal/molecule hybridization on the effective polarization has been proposed to explain these results.[8] However, to fully exploit this effect, a comprehensive understanding down to the molecular scale is still a major and challenging issue.[9,10] Spin-polarized scanning tunneling microscopy/spectroscopy (SP-STM/STS) is a unique tool to measure the spin polarization of surfaces, nanostructures, and molecules at the atomic scale and is therefore a powerful technique to probe the effect of contacting a molecule to a magnetic surface. When an organic molecule is brought into contact with a metallic electrode, its molecular levels are generally broadened and shifted depending on the geometrical and electronic details of the contact. In the case of a magnetic electrode, these broadening and shifting are in principle spin-dependent, leading finally to a spin-polarized density of states of the molecule itself.[8,11,12] Using SP-STM, two experiments have recently shown a spin contrast through single magnetic molecules.[10,13] On nonmagnetic molecules, a spin contrast could also be observed at energies close to the Fermi level.[12,14] However, the experimental evidence of the spin polarization of molecular orbitals by hybridization with a magnetic substrate is still lacking.

C_{60} is a promising molecule for spintronic applications due to its weak intrinsic spin−orbit interaction[15] together with the zero nuclear spin of the majority ^{12}C isotope of carbon that avoids hyperfine interaction. Furthermore this latter is another source of spin relaxation generally occurring in organic molecules due to hydrogen atoms. The potential of C_{60} for molecular spintronics has been recently emphasized by the demonstration of the spin polarization of the molecular orbitals of C_{60} adsorbed onto a Fe layer[16] and the realization of a C_{60} based room-temperature spin valve device.[17] After depositing such molecules on a Cr(001) substrate, we measured molecular orbitals of C_{60} adsorbed on terraces with opposite magnetization and compared it with spin-resolved ab initio calculations, demonstrating a strong spin splitting of the lowest unoccupied molecular orbital. Our work, that is, the first investigation of C_{60} molecules on a magnetic surface using SP-STM/STS, provides for the first time the experimental evidence of a spin splitting of a molecular orbital through a complete spin-polarized spectroscopic study at the single molecule level.

Received: May 13, 2012
Revised: July 9, 2012

dx.doi.org/10.1021/nl301802e | *Nano Lett.* XXXX, XXX, XXX−XXX

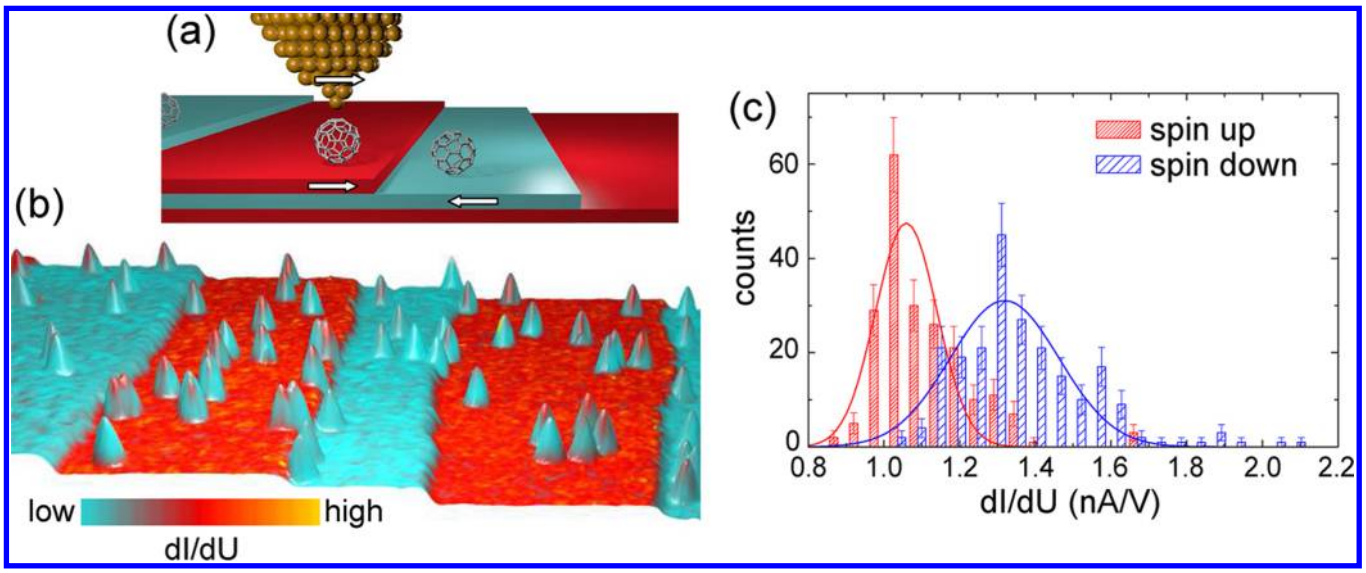

Figure 1. (a) Schematic view of the STM junction. A magnetic tip is used to measure the transport through C_{60} molecules adsorbed on antiferromagnetically ordered terraces of the Cr(001) surface. (b) 100 × 65 nm^2 three-dimensional composite of topographic STM image (U = 1 V, I = 300 pA) colored with spin-resolved dI/dU map at U = −25 mV measured with open feedback loop (starting from the set point of the topography). Two levels of differential conductance can be seen above adjacent terraces of the chromium sample. C_{60} molecules exhibit positively correlated levels of conductance on both types of terraces at this voltage. (c) Statistical dispersion of the dI/dU signal measured above the center of 427 individual molecules, about half of which were adsorbed, respectively, on the "up" and "down" terraces (closed feedback loop at −0.5 V).

This clearly shows the way toward a molecular engineering of magnetoresistance for spintronics.

Experiments were conducted using a low temperature STM (5 K) under UHV conditions (less than 10^{-11} mbar). The chromium sample was prepared by repeated Ar^+ ions sputtering (2 keV) and annealing (900 K) cycles and then placed on the STM stage. Fullerene molecules were then deposited in situ onto the cold sample from a C_{60} powder sublimated in a crucible resistively heated at 600 K. A sparse distribution of single molecules onto the surface is obtained with all possible polar and azimuthal orientations. A subsequent annealing at room temperature makes almost all molecules turn into a pentagonal adsorption geometry. The magnetic Fe/W tip was prepared using an electrochemically etched tungsten tip shortly annealed under UHV, and then around 40 monolayers of iron were evaporated onto the tip apex. Differential conductance spectra were acquired using lock-in detection with a modulation signal at 750 Hz and 25 mV.

Our model system consists of single C_{60} molecules deposited on a Cr(001) surface under ultrahigh vacuum (UHV) and probed with a magnetic tip (Figure 1a). SP-STM allows to measure the local tunneling magnetoresistance (TMR) above each single molecule at the atomic scale. Typical SP-STM images are obtained as shown in Figure 1b where a topographic STM image has been mapped with the differential conductance signal (dI/dU, color coded) at −25 mV. Adjacent terraces of the Cr(001) surface exhibit alternating high and low conductance levels revealing two in-plane opposite magnetizations of adjacent chromium layers due to the antiferromagnetic order in the [001] direction.[18] We will refer to these as "up" and "down" terraces arbitrarily. A careful look of the conductance values at the center of the molecules shows a striking correlation with the TMR between chromium terraces. We also observed the same phenomena at −0.5 V but with an inversion of the molecular TMR with respect to the chromium TMR.

To measure quantitatively the TMR, we report on typical dispersion histograms of the dI/dU signal measured above the center of molecules at U = −0.5 V on both terraces, and a Gaussian fit of each histogram, as seen in Figure 1c. This statistical measurement was repeated with several tip states and constantly yields the same order of magnitude of both TMR and width of the distributions. These dispersions that widely exceed the energy resolution of the measurement may be explained by the presence of impurity defects on the Cr(001) surface[19] and by the different azimuthal orientations of the molecules. The role of impurities on the local electronic and magnetic properties of the C_{60} molecules is still unclear, but we expect that it should concern only a few molecules in our sample due to a low concentration of surface impurities. However, the histogram of Figure 1c clearly shows a difference in the mean value of the differential conductances on the two sets of data that largely overcomes the dispersion measured on each terrace. We calculated the corresponding TMR using the standard definition based on the Julliere model:[20]

$$\mathrm{TMR} = \frac{(\mathrm{d}I/\mathrm{d}U)_{\mathrm{up}} - (\mathrm{d}I/\mathrm{d}U)_{\mathrm{down}}}{(\mathrm{d}I/\mathrm{d}U)_{\mathrm{down}}} \quad (1)$$

It is worthy to note that the tip and sample magnetizations being in plane, their relative orientation may be tilted and not collinear, which would lead to an underestimation of the TMR. The measurements of Figure 1c yield a TMR value of −30%. One should note that in this experiment we use the intensity of the dI/dU signal at −0.5 V measured in a topographic image obtained at the same bias voltage. This may weaken the measured effect because the constant current imaging may compensate the dI/dU differences.[19]

A comprehensive understanding of the energy resolved spin transport through the C_{60} molecules is provided by an energy-dependent analysis of the magnetic contrast. In Figure 2a we report averaged spin-resolved tunneling spectra measured above the center of 16 C_{60} molecules adsorbed on a pentagon

dx.doi.org/10.1021/nl301802e | Nano Lett. XXXX, XXX, XXX−XXX

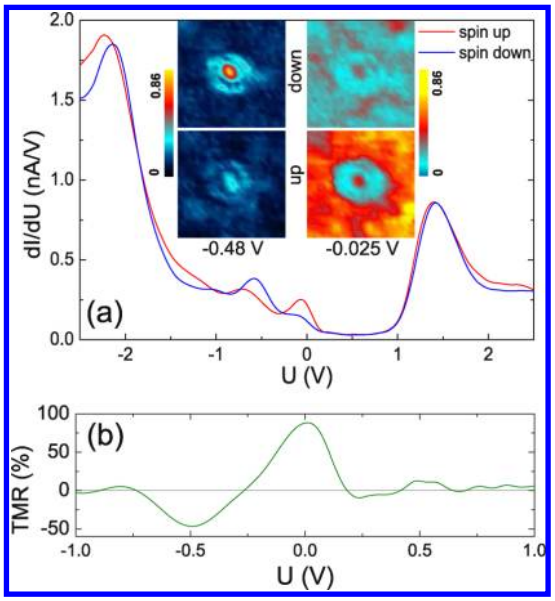

Figure 2. (a) dI/dU spectra locally measured above the center of molecules on "spin up" and "spin down" terraces (starting from a set point U = 1 V). Each spectrum is an average over 16 molecules. The insets show the conductance maps measured over two molecules on "spin up" and "spin down" terraces with an open feedback loop (set point before opening the loop, U = 1 V, I = 300 pA). The maximum signal of 0.86 nA/V in the insets is to be compared with the maximum of the averaged spectra and illustrates the important dispersion of the dI/dU values (see Figure 1c). The sign of the TMR above Cr(001) is positive at both energies. (b) Magnetoresistance calculated from part a between −1 V and +1 V.

on the two types of terraces. The resonances around −2 V and +1.4 V can be assigned to the highest occupied (HOMO) and second lowest unoccupied (LUMO) molecular states of the free molecule (free molecule HOMO and LUMO+1, respectively) following the calculations which will be presented later in the paper. At −0.5 V a clear difference is observed between spectra obtained above C_{60} on spin up and spin down terraces. This observation reveals the spin polarization of this state. It is consistent with the above TMR measurement at this voltage. The spatial dependence on the spin polarization can be revealed by comparing the dI/dU maps of molecules adsorbed on spin up and down terraces. Such spin sensitive spatial mapping is reported in the inset of Figure 2a. It shows that the local density of states (LDOS) of this molecular state attributed to the LUMO state has a different intensity depending on the magnetization orientation of the terrace with an intense contrast above the center of the molecule. Local spectra also exhibit another peak near the Fermi level, which is also spin-polarized, but with an opposite sign compared to the one at −0.5 V.

We can extract values of the TMR calculated from the spectra in Figure 2a using eq 1. They are reported in Figure 2b. It shows that TMR values up to 100% can be achieved through C_{60} molecules. Moreover, the sign of the TMR is inverted at −0.5 V compared to the TMR at the Fermi level. At this stage a crucial question is whether the two peaks at −0.5 V and at the Fermi level correspond to two different molecular orbitals. A LUMO splitting was observed by STS on C_{60} on Ag(100).[21,22] In this case the corresponding dI/dU maps exhibit different patterns. Here we do not observe such variations. On the contrary the dI/dU map is persistent over a broad range of energy from −1 V to E_F and for both spin channels. Therefore we believe that these two peaks can be ascribed to the same molecular state. Indeed the comparison with ab initio simulations detailed below will allow to attribute these two peaks to the single m = 0 LUMO orbital.

We have carried out ab initio density-functional theory (DFT) electronic structure calculations using plane-waves package Quantum-ESPRESSO[23] within the generalized gradient approximation (GGA) for exchange-correlation functionals in the Perdew, Burke, and Ernzerhof parametrization.[24] One should mention that we are aware of rather poor description of Cr by GGA, in particular, the overestimation of the magnetic moment of Cr(001) surface;[25] to improve results one often needs to suppress the surface magnetism in some way. We find, however, that in our case of C_{60}/Cr(001) the GGA works pretty well allowing for a reasonably good theoretical interpretation of experimental data. One of the reasons of good performance of GGA could be a very strong reduction of the Cr surface magnetism by adsorbed C_{60} molecules: the magnetic moment of Cr atom right beneath the molecule is reduced more than three times with respect to the clean Cr surface (see the Supporting Information). We can simulate theoretically energy-resolved spectral maps by calculating the LDOS at the energy of interest on the isosurface of LDOS integrated from zero to that energy (simulating the STM topograph).[21,26] This allows to take into account the possible influence of the topography on the conductance map that could have an impact on the exact shape measured in the conductance map. Such images are shown in Figure 3 (for down spin polarization) at U = −1.4, −0.4, and

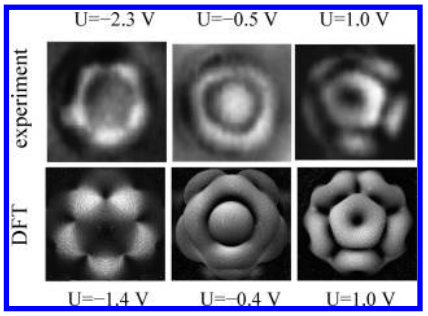

Figure 3. Top row: experimental dI/dU maps (closed loop) at U = −2.3 V, −0.5 V, and 1.0 V. The −0.5 V map remains the same up to the Fermi level. Bottom row: simulated DFT dI/dU maps for spin down channel (the results for up spin are qualitatively similar) at U = −1.4 V, −0.4 V, and 1.0 V, showing the signatures of HOMO, LUMO m = 0, and LUMO+1 molecular orbitals, respectively.

1.0 V. These images are compared to experimental energy resolved spectral mapping of the dI/dU signal at bias voltages corresponding to the peaks observed in the dI/dU spectra. This is reported in Figure 3 top row. We find a good agreement between theoretical and experimental images, except of the shift of the HOMO peak (see the following discussion): we observe five bright spots coming from the hexagon atoms in the HOMO image (U = −1.4 V), a bright circle at the pentagon center, characteristic for the m = 0 LUMO orbital (U = −0.4 V), and, on the contrary, a bright ring with a dark central part for the LUMO+1 image (U = 1.0 V). Note that the latter change of contrast between LUMO and LUMO+1 states was already reported for C_{60} molecules adsorbed on Ag(100).[21,22]

dx.doi.org/10.1021/nl301802e | Nano Lett. XXXX, XXX, XXX−XXX

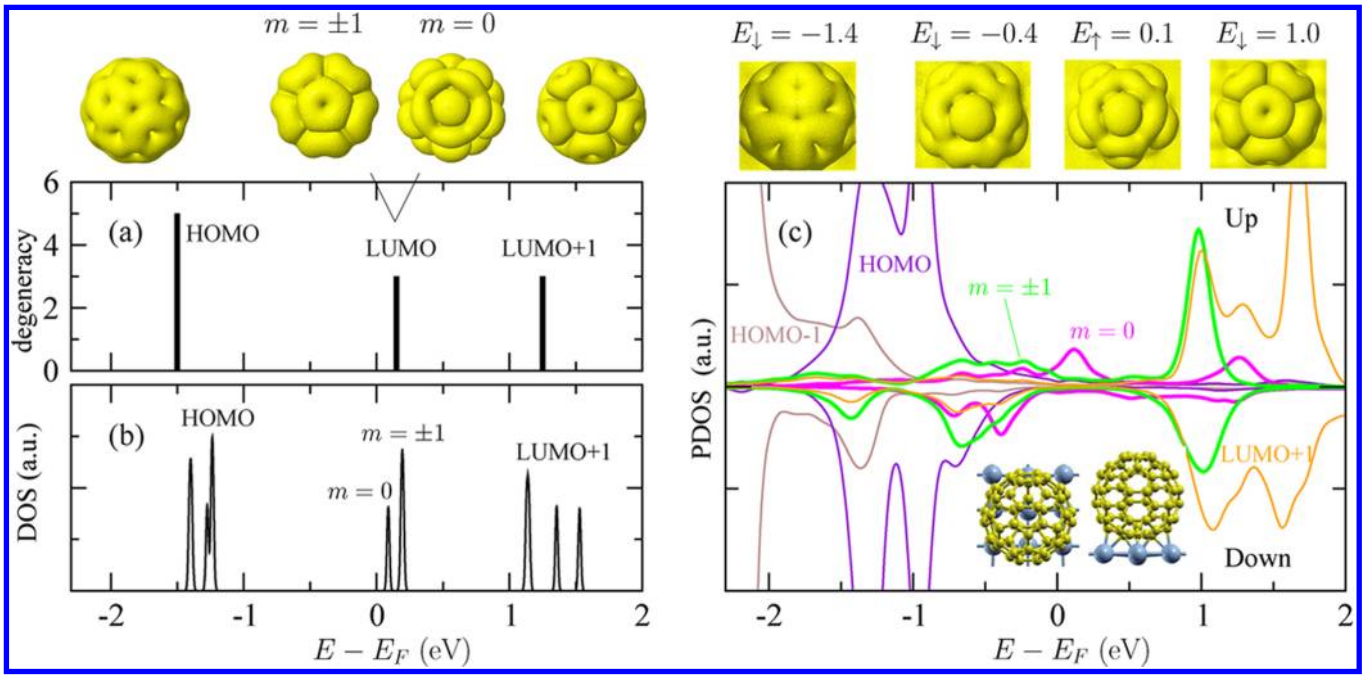

Figure 4. DFT calculations: (a) free C_{60} molecule: energy levels and their degeneracies; (b) DOS of free but distorted (as after deposition on the Cr surface) C_{60} molecule. (c) C_{60} on Cr(001) (see inset): DOS projected on different molecular orbitals of deformed molecule for both spin polarizations. The magnetic moment of Cr surface layer specifies the "up" direction; we also plot the down spin wave functions at some selected energies corresponding to HOMO, LUMO $m = 0$ (both spins are shown), and LUMO+1 hybridized states.

As a reference with an isolated C_{60} molecule, we show the DFT eigenvalues, degeneracies, and spatial distributions of HOMO, LUMO, and LUMO+1 molecular orbitals, in Figure 4a, which agree well with previous results.[21] All of the levels can be labeled by an integer number m reflecting their symmetry with respect to a 5-fold rotational axis passing through the centers of two opposite pentagons and perpendicular to the page in Figure 4a. In particular, the three LUMO states are of $m = \pm 1$ and $m = 0$ symmetry and have very different spatial distributions: the $m = \pm 1$ orbitals are localized on the pentagon ring, while the $m = 0$ orbital is rather circular with the maximum extension at the pentagon center. Therefore the observed molecular orbitals at −0.5 V seem to be characteristic for $m = 0$ LUMO orbital.

To demonstrate the link between the molecular orbitals of the C_{60} modified by the interface with the chromium surface and the inversion of sign of the TMR reported above, we now turn to the electronic structure of our whole system, namely, the C_{60} molecules deposited on the chromium surface. The Cr surface was simulated by five (001) atomic layers, and the (4×4) in-plane periodicity of the supercell was used. The plane wave cut-offs were 30 and 300 Ry for the wave functions and for the charge density, respectively. Integration over irreducible Brillouin zone was accomplished using a $(4 \times 4 \times 1)$ mesh of k-points and a smearing parameter of 10 mRy. The C_{60} molecule and the two Cr surface layers were allowed to relax, while the other Cr layers were kept at their bulk positions. Electronic structure of the relaxed system has been further refined using more k-points ($(8 \times 8 \times 1)$ k-point mesh) and 11 layers of Cr. The shape of the molecular orbitals observed experimentally indicates that the C_{60} molecule is adsorbed on the Cr surface by the pentagon ring. Taking this into account in the calculations, several adsorption sites were studied. It was found that the molecule binds most strongly at atop the adsorption site (the pentagon center above the Cr atom as depicted on the inset of Figure 4c) with the large adsorption energy of 3.9 eV and the shortest C−Cr distance of about 2 Å. We note that at such a strong binding the effects of van der Waals interactions are negligible (see the Supporting Information). As a result of strong binding, the C_{60} molecule becomes distorted: in particular, its bottom gets much flattened, providing more bonds to the substrate (see the inset of Figure 4c).

It has been found that the strong binding of C_{60} molecule to Cr surface affects dramatically its molecular orbitals. This effect has two sources: the strong distortion of the molecule and the coupling of molecular states to the substrate states. We first analyze the effect of distortion alone showing in Figure 4b the DOS of free but distorted C_{60} molecule. The (degenerated) HOMO, LUMO, and LUMO+1 orbitals get split and shifted in energy. In particular, the LUMO levels split into $m = 0$ and almost degenerate pair of $m = \pm 1$ states, while the HOMO states move to higher energies thus decreasing the LUMO−HOMO gap by about 0.4 eV. Rather interestingly, one more state appears near the LUMO+1 states, at the energy of 1.5 eV. It originates from higher-energy states and has a spatial shape similar to the LUMO $m = 0$ orbital. All of the levels are of course spin-degenerate.

Our calculations show that, when the molecule is further brought in contact with the Cr surface, the up and down molecular orbitals hybridize very differently with the substrate states. This is especially true for the LUMO orbitals (mainly localized on pentagons) and could be due to rather different up/down DOS of a clean Cr surface around the Fermi energy: the spin up DOS is much larger (possibly due to the presence of spin up surface state) than the spin down one. Figure 4c shows the up and down DOS of the whole C_{60}/Cr(001) system projected onto different molecular orbitals of free deformed C_{60} molecule (the "up" direction refers to the magnetic moment of Cr surface layer). Near the Fermi energy one can clearly see the

dx.doi.org/10.1021/nl301802e | Nano Lett. XXXX, XXX, XXX−XXX

spin-split LUMO $m = 0$ resonances appearing at 0.1 eV for up spin and at −0.4 eV for down spin channels. The LUMO $m = \pm 1$ states do not show such a pronounced spin-splitting and appear partially at negative energies (broad features around −0.5 eV) and at positive energies (around 1 eV), mixing with the LUMO+1 states having the similar spatial shape. We notice also that both HOMO-1 and HOMO derived states are shifted to positive energies so that the HOMO-1 main peak appears right at the left boundary of the figure, at $E < -2$ eV (the HOMO-1 states for an isolated molecule were out of energy range of the figure). Note that PDOS shown in Figure 4c suggest significant charge transfer to the molecule and its negative (opposite to the Cr surface layer, a kind of antiferromagnetic coupling) spin polarization (for detailed discussion, see the Supporting Information).

The PDOS analysis done above does not allow to make a direct comparison with STS data since it does not take into account the spatial shape of electron wave functions and their decay in the vacuum where the STM tip is located. Instead, the so-called vacuum LDOS appears in a spin-polarized version of well-known Tersoff−Hamann approach to tunneling differential conductance:[27]

$$G = \frac{dI}{dU} \propto \sum_{\sigma} n_T^{\sigma} n_S^{\sigma}(R_T, E_F + eU) \tag{2}$$

where n_T^{σ} are spin-dependent tip DOS (assumed to be constant in energy), and

$$n_S^{\sigma}(R_T, E_F + eU) = \sum_j |\psi_{Sj}^{\sigma}(R_T)|^2 \delta(\varepsilon_j - E_F - eU) \tag{3}$$

is the spin-dependent vacuum LDOS of the substrate (the surface plus the molecule) at the tip position R_T and at the applied voltage U.

We plot therefore in Figure 5a the vacuum LDOS at 6 Å above the pentagon center for both up (solid blue lines) and down (solid red lines) spin polarizations (which is calculated by integrating $n_S^{\sigma}(R_T, E)$ inside a small cube of size 0.4 Å). We observe that around the Fermi energy the both curves follow very closely the LUMO $m = 0$ DOS, showing in particular the two rather narrow peaks at 0.1 eV (spin up) and −0.4 eV (spin down). In the case of fully spin-polarized tip (e.g., $n_T^{\uparrow} = 0$, $n_T^{\downarrow} \neq 0$), these two vacuum LDOS may be directly compared with two differential conductance curves in Figure 2a due to eq 2. For more realistic case of partially polarized tip ($n_T^{\uparrow} \neq 0$, $n_T^{\downarrow} \neq 0$), two vacuum LDOS will be mixed together in different proportions (related to the tip polarization). In any case, the two LUMO related features in the vacuum LDOS around the Fermi energy seem to match pretty well to the two low bias peaks observed in STS experiments. Also in agreement with experiment, we observe a large increase in vacuum LDOS at $E > 1$ eV which is in fact related to the LUMO+1 states. On the contrary, the HOMO states are almost invisible due to probably their localization on the pentagon-hexagon bonds, while the vacuum LDOS is probed above the pentagon center. They will indeed show up if the LDOS is taken above the pentagon atoms as is shown (after averaging over different pentagon atoms) in Figure 5a by dashed lines. Well-pronounced (especially for spin down channel) features appear now at the energy around −1.4 eV. We associate these features to the STS peak observed at $U = -2$ V since our theoretical and experimental spectral maps match very nicely as can be seen from the left column of Figure 3. A much bigger height of the experimental peak could be explained by several reasons: a more massive STM tip probing the states in much bigger space region, not only at the pentagon center; the deformation of the tunneling barrier at this large voltage leading to the increase of the tunneling current; and, finally, the increase in the Fe tip DOS for unoccupied (spin down) states breaking the applicability of the Tersoff−Hamann model. Another problem is the shift in energy of the HOMO-related peak by about 1 V which could be related to the usual failure of the mean-field DFT approach in describing properly the position of molecular levels and thus the underestimation of the LUMO−HOMO gap. It should be also noted that the vacuum (spin down) LDOS shows a small peak at about −2.2 eV due to HOMO-1 derived states. We do not however associate this peak to the experimental peak at −2 V since the theoretical spectral maps turn out to be rotated by an angle of $\pi/5$ with respect to the experimental map (see the Supporting Information). Finally, we have calculated the spin polarization of the LDOS above the pentagon center (Figure 5b). At the energies of the spin-down and spin-up LUMO $m = 0$ state (−0.4 and 0.1 eV), the spin polarization exhibits maxima, and the sign of the spin polarization changes from negative to positive values. Therefore, the voltage-dependent experimental TMR, and in particular the sign inversion, reported in Figure 2 can be attributed to the variation of the spin polarization of the LDOS above the molecule. It is worth noting that at large bias the experimental TMR vanishes, in contrary to the calculated spin polarization. This could be due to spin flip process occurring at high energy that is not taken into account in the calculations.

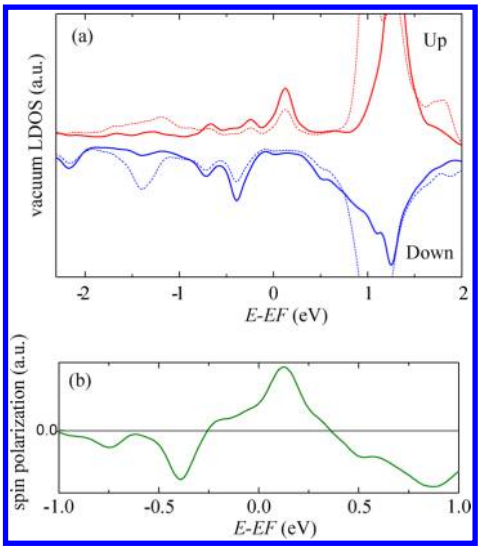

Figure 5. DFT calculations: (a) vacuum DOS at 6 Å right above the pentagon center (solid lines) and above the pentagon atoms (dashed lines). In the last case the DOS was averaged over different pentagon atoms. (b) Spin polarization calculated from the difference between the spin up and the spin down LDOS above the pentagon center.

In summary, it has been found that single C_{60} molecules strongly interact with a Cr(001) surface in the pentagonal adsorption geometry. This interaction induces the spin-splitting of a LUMO derived state close to the Fermi energy which, as confirmed by DFT calculations, can be probed by STS far away from the Cr surface. Various molecular states of the interacting molecule have been imaged at different voltages using STS with an intramolecular resolution and have been reasonably well-reproduced by DFT simulations. Present SP-STS measure-

dx.doi.org/10.1021/nl301802e | Nano Lett. XXXX, XXX, XXX−XXX

ments are the first ones achieved on a full carbon, nonplanar molecule. This study has shown that the molecules acquire a spin-polarized DOS at molecular resonances, which is both energy and spatially dependent and can be strongly amplified and inversed with respect to the Cr surface. This result opens the way to an engineering of spin filtering through molecular orbitals.

■ ASSOCIATED CONTENT

Supporting Information

Technical details on the measurement of dI/dU maps, van der Waals interactions, charge transfer, spin polarization, and conductance map rotation between HOMO and HOMO-1 orbitals. This material is available free of charge via the Internet at http://pubs.acs.org.

■ AUTHOR INFORMATION

Corresponding Author

*E-mail: jerome.lagoute@univ-paris-diderot.fr.

Notes

The authors declare no competing financial interest.

■ ACKNOWLEDGMENTS

We would like to thank the Conseil Régional Ile-de-France for funding. V.R. acknowledges Institut Universitaire de France for support.

■ REFERENCES

(1) Tedrow, P.; Meservey, R. *Phys. Rev. Lett.* **1971**, *26*, 192.
(2) Baibich, M. N.; Broto, J. M.; Fert, A.; Van Dau, F. N.; Petroff, F.; Etienne, P.; Creuzet, G.; Friederich, A.; Chazelas, J. *Phys. Rev. Lett.* **1988**, *61*, 2472−2475.
(3) Miao, G.-X.; Münzenberg, M.; Moodera, J. S. *Rep. Prog. Phys.* **2011**, *74*, 036501.
(4) Lou, X.; Adelmann, C.; Crooker, S. A.; Garlid, E. S.; Zhang, J.; Reddy, K. S. M.; Flexner, S. D.; Palmstrøm, C. J.; Crowell, P. A. *Nat. Phys.* **2007**, *3*, 197−202.
(5) Awschalom, D. D.; Flatté, M. E. *Nat. Phys.* **2007**, *3*, 153−159.
(6) Naber, W. J. M.; Faez, S.; van der Wiel, W. G. *J. Phys. D: Appl. Phys.* **2007**, *40*, R205−R228.
(7) Dediu, V. A.; Hueso, L. E.; Bergenti, I.; Taliani, C. *Nat. Mater.* **2009**, *8*, 707−716.
(8) Barraud, C.; Seneor, P.; Mattana, R.; Fusil, S.; Bouzehouane, K.; Deranlot, C.; Graziosi, P.; Hueso, L.; Bergenti, I.; Dediu, V.; Petroff, F.; Fert, A. *Nat. Phys.* **2010**, *6*, 615−620.
(9) Rocha, A. R.; Garca-Suárez, V. M.; Bailey, S. W.; Lambert, C. J.; Ferrer, J.; Sanvito, S. *Nat. Mater.* **2005**, *4*, 335−339.
(10) Brede, J.; Atodiresei, N.; Kuck, S.; Lazić, P.; Caciuc, V.; Morikawa, Y.; Hoffmann, G.; Blügel, S.; Wiesendanger, R. *Phys. Rev. Lett.* **2010**, *105*, 047204.
(11) Sanvito, S. *Nat. Phys.* **2010**, *6*, 562−564.
(12) Atodiresei, N.; Brede, J.; Lazić, P.; Caciuc, V.; Hoffmann, G.; Wiesendanger, R.; Blügel, S. *Phys. Rev. Lett.* **2010**, *105*, 066601.
(13) Iacovita, C.; Rastei, M.; Heinrich, B.; Brumme, T.; Kortus, J.; Limot, L.; Bucher, J. *Phys. Rev. Lett.* **2008**, *101*, 116602.
(14) Schmaus, S.; Bagrets, A.; Nahas, Y.; Yamada, T. K.; Bork, A.; Bowen, M.; Beaurepaire, E.; Evers, F.; Wulfhekel, W. *Nat. Nanotechnol.* **2011**, *6*, 185−189.
(15) Huertas-Hernando, D.; Guinea, F.; Brataas, A. *Phys. Rev. B* **2006**, *74*, 155426.
(16) Tran, T.; Wong, P.; De Jong, M.; Van Der Wiel, W.; Zhan, Y.; Fahlman, M. *Appl. Phys. Lett.* **2011**, *98*, 222505.
(17) Gobbi, M.; Golmar, F.; Llopis, R.; Casanova, F.; Hueso, L. E. *Adv. Mater.* **2011**, *23*, 1609−1613.
(18) Wiesendanger, R.; Güntherodt, H.-J.; Güntherodt, G.; Gambino, R.; Ruf, R. *Phys. Rev. Lett.* **1990**, *65*, 247−250.
(19) Lagoute, J.; Kawahara, S. L.; Chacon, C.; Repain, V.; Girard, Y.; Rousset, S. *J. Phys.: Condens. Matter* **2011**, *23*, 045007.
(20) Julliere, M. *Phys. Lett. A* **1975**, *54*, 225−226.
(21) Lu, X.; Grobis, M.; Khoo, K.; Louie, S.; Crommie, M. *Phys. Rev. Lett.* **2003**, *90*, 7−10.
(22) Lu, X.; Grobis, M.; Khoo, K.; Louie, S.; Crommie, M. *Phys. Rev. B* **2004**, *70*, 1−8.
(23) Giannozzi, P.; et al. *J. Phys.: Condens. Matter* **2009**, *21*, 395502.
(24) Perdew, J. P.; Burke, K.; Ernzerhof, M. *Phys. Rev. Lett.* **1996**, *77*, 3865−3868.
(25) Bihlmayer, G.; Asada, T.; Blügel, S. *Phys. Rev. B* **2000**, *62*, R11937−R11940.
(26) Larsson, J.; Elliott, S.; Greer, J.; Repp, J.; Meyer, G.; Allenspach, R. *Phys. Rev. B* **2008**, *77*, 115434.
(27) Wortmann, D.; Heinze, S.; Kurz, P.; Bihlmayer, G.; Blügel, S. *Phys. Rev. Lett.* **2001**, *86*, 4132−4135.